α-RgIA: A Novel Conotoxin That Specifically and Potently Blocks the α9α10 nAChR[†,‡]

Michael Ellison,*[,§] Christian Haberlandt,[§] María Eugenia Gomez-Casati,[||] Maren Watkins,[⊥] A. Belén Elgoyhen,[||] J. Michael McIntosh,[#] and Baldomero M. Olivera[§]

Departments of Biology, Pathology, and Psychiatry, University of Utah, Salt Lake City, Utah 84112, and Instituto Investigaciones en Ingeniería Genética y Biología Molecular, Consejo Nacional de Investigaciones Científicas y Técnicas-Universidad de Buenos Aires, Buenos Aires 1428, Argentina

Received October 4, 2005; Revised Manuscript Received November 14, 2005

ABSTRACT: The α9 and α10 nicotinic acetylcholine receptor (nAChR) subunits assemble to form the α9α10 nAChR subtype. This receptor is believed to mediate cholinergic synaptic transmission between efferent olivocochlear fibers and the hair cells of the cochlea. In addition α9 and/or α10 expression has been described in dorsal root ganglion neurons, lymphocytes, skin keratinocytes, and the pars tuberalis of the pituitary. Specific antagonists that selectively block the α9α10 channel could be valuable tools for elucidating its role in these diverse tissues. This study describes a novel α-conotoxin from the Western Atlantic species *Conus regius*, α-conotoxin RgIA (α-RgIA), that is a subtype specific blocker of the α9α10 nAChR. α-RgIA belongs to the α4/3 subfamily of the α-conotoxin family; sequence and subtype specificity comparisons between α-RgIA and previously characterized α4/3 toxins indicate that the amino acids in the C-terminal half of α-RgIA are responsible for its preferential inhibition of the α9α10 nAChR subtype.

Predatory marine snails in the genus *Conus* have venoms that are rich in neuropharmacologically active peptides (*1*−*6*). There are approximately 500 species in *Conus*, and among those that have been examined so far, a conserved feature is the presence of α-conotoxins in their venom. These are highly disulfide cross-linked peptides with the disulfide scaffold shown in Figure 1; due to high sequence variability of their non-cysteine residues α-conotoxins are extremely diverse and each *Conus* species has a unique complement of α-conotoxins. α-Conotoxins are synthesized as large precursors, and the mature toxin is generated by a proteolytic cleavage toward the C-terminus of the precursor. In contrast to the variable inter-cysteine sequences of the mature toxins, the precursors and the genes encoding them are quite conserved both among α-conotoxins in a given *Conus* species and from species to species. α-Conotoxins have generally been shown to be nicotinic acetylcoline receptor (nAChR) antagonists (*6*−*9*).

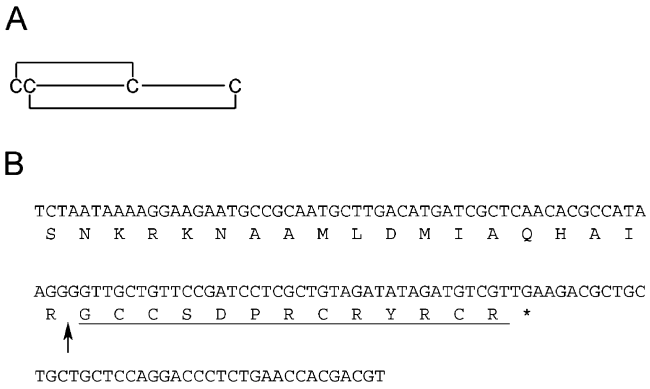

FIGURE 1: Primary structure and disulfide scaffold of α-RgIA. A. The characteristic disulfide scaffold of the α-conotoxins. B. The cloned fragment of the α-RgIA precursor gene and the predicted translation product. The putative mature toxin (underlined) is assumed to be defined by a proteolytic processing site (indicated by the arrow) to the C-terminal side of an arginine residue and the stop codon (represented by the asterisk) at the C-terminal of the precursor.

nAChRs are a group of acetylcholine gated ion channels that are part of the ligand gated ion channel superfamily (*10, 11*). They are pentamers of transmembrane subunits surrounding a central ion conducting channel. Many different subunits have been identified, and most fall into two main subfamilies (the α subunits and the β subunits). The subunits can associate in various combinations in the receptor pentamers, leading to a diverse family of receptor subtypes. Most of the subtypes contain subunits from both the α and β subunit families, e.g., the human adult muscle subtype contains two α1 subunits and a β1 subunit (in addition to a δ and an ϵ subunit) and the α3β2 subtype is composed of

[†] This work was supported by an International Research Scholar grant from the Howard Hughes Medical Institute, the Agencia Nacional de Promoción Científica y Tecnológica, the University of Buenos Aires (A.B.E.), and National Institutes of Health Grants GM48677 and MH53631.

[‡] The sequence of the fragment of the α-RgIA precursor gene has been deposited at GenBank (accession code DQ239610).

* To whom correspondence should be addressed. Mailing address: Department of Biology, University of Utah, 257 South 1400 East, Salt Lake City, UT 84112-0840. Tel: (801) 581-8370. Fax: (801) 585-5010. E-mail: michael.ellison@m.cc.utah.edu.

[§] Department of Biology, University of Utah.

[||] Consejo Nacional de Investigaciones Científicas y Técnicas-Universidad de Buenos Aires.

[⊥] Department of Pathology, University of Utah.

[#] Department of Psychiatry, University of Utah.

10.1021/bi0520129 CCC: $33.50
Published on Web 01/13/2006

α3 and β2 subunits. nAChRs that are composed of only α subunits are the α7 and α9 subtypes (homopentamers) and the α9α10 subtype (an all α heteropentamer). Phylogenetic analysis shows that the α7, α9, and α10 subunits are more closely related to each other than they are to other nAChR subunits (*12*, *13*).

The α9 and α10 nAChR subunits are expressed in diverse tissues. In the inner ear α9α10 nAChRs mediate synaptic transmission between efferent olivocochlear fibers and cochlear hair cells (*13*−*15*). The α9 and α10 subunits are also found in dorsal root ganglion neurons (*16*, *17*), lymphocytes (*18*), skin keratinocytes (*19*−*21*), and the pars tuberalis of the pituitary (*13*−*15*). Specific antagonists of the α9α10 nAChR could be useful tools for elucidating the receptor's role in these various locations. This study describes the discovery and initial characterization of a novel α9α10 subtype specific antagonist, α-conotoxin RgIA (α-RgIA[1]).

MATERIALS AND METHODS

Cloning of the Mature Toxin Region of α*-RgIA.* The hepatopancreas was isolated from a specimen of *Conus regius* and was stored at −70 °C. Genomic DNA was extracted from the tissue using Puregene reagents and the marine invertebrates protocol provided by the manufacturer (Gentra). As described previously (*22*, *23*) the DNA was used as the template in PCR reactions where the primers anneal to conserved regions of α-conotoxin genes and thus amplify α-conotoxin gene fragments that include the mature toxin region. The resulting mixed pool of PCR products (corresponding to different *C. regius* α-conotoxins) was gel purified and used as the insert DNA for the CloneAmp system (Life Technologies/GibcoBRL). Resulting pAMP1 based plasmids were transformed into competent DH5α, and plasmid DNA was purified from multiple clones. The sequence of the inserts in these plasmids was obtained at a University of Utah core facility.

Preparation of Synthetic α*-Conotoxins.* Linear α-RgIA was synthesized by standard Fmoc chemistry using an ABI 430A peptide synthesizer at a University of Utah core facility. The peptide was oxidized to give the correct disulfide connectivity (first cysteine to third cysteine and second cysteine to fourth cysteine) using orthogonal cysteine protection. The first and third cysteine residues were incorporated with acid labile *S*-trityl protection whereas the second and fourth cysteine residues had stable *S*-acetamidomethyl protection. This allowed a previously described scheme (*24*) to be used to sequentially close the first cysteine to third cysteine and then the second cysteine to fourth cysteine disulfide bridges. Synthetic α-ImI was prepared as described before (*25*).

Xenopus oocyte Electrophysiology. Previously described (*14*, *15*, *26*, *27*) clones of rat nAChR subunits were used to prepare the corresponding cRNAs as described before (*28*). Functional nAChRs were expressed on *Xenopus* oocytes by injection of the appropriate cRNAs as described previously (*14*, *15*, *26*, *27*). Oocytes were maintained in a 30 μL cylindrical recording chamber made from Sylgard and were gravity perfused at a rate of approximately 1 mL/min with ND96A (96.0 mM NaCl, 2.0 mM KCl, 1.8 mM $CaCl_2$, 1.0 mM $MgCl_2$, 5 mM HEPES, pH 7.5, 1 μM atropine). The perfusion medium could be switched to one composed of ND96A plus ACh using a series of three-way solenoid valves as described previously (*26*).

Oocytes were voltage clamped at −70 mV using a two-electrode voltage clamp. Details of the voltage clamp apparatus have been described previously (*26*). Electrical currents were gated by 1-s applications of ACh at 1-min intervals. The ACh concentration was close to the EC50 for each subtype (200 μM ACh for α7 receptors, 10 μM for α9α10 receptors, and 100 μM ACh for all the other subtypes). The currents were digitally recorded as described before (*26*). Only oocytes that gave consistent currents in response to the sequential ACh applications were used in experiments. Because α9α10 receptors have been shown to conduct large amounts of Ca^{2+} (*15*) and thus activate large Ca^{2+} gated Cl^- currents in oocytes, the inhibition of ACh gated currents by α-RgIA were measured as described above and using oocytes that had been placed in ND96 containing BAPTA-AM (100 μM) overnight prior to use. Recordings were made at room temperature (22−25 °C).

To measure inhibition by conotoxins ND96A perfusion and ACh pulses were stopped. Peptide dissolved in ND96A was then manually applied to the static buffer in the recording chamber, and after 5 min ND96A flow was restarted at the same time as an ACh pulse was applied. For each application of conotoxin the peak current gated by the first ACh pulse after toxin application was expressed as a percentage (% response) of the corresponding peak in control experiments where ND96A (instead of toxin) was applied. Toxin was not included in the ACh pulses because of the brief time (<2 s) that it took for the ACh gated currents to peak; it was thus assumed that only minimal amounts of receptor bound toxin could dissociate prior to the first peak current after toxin application. Also, in the recording chamber the bolus of ACh does not directly project onto the oocyte; instead it enters tangentially and then swirls and mixes with the bath solution; given the flow rate of liquid through the recording chamber this results in the toxin concentration in the recording chamber remaining high (>50% of the concentration originally in the bath) until after the ACh response has peaked.

Recordings from Inner Hair Cells. Apical turns of the organ of Corti were excised from Sprague−Dawley rats at postnatal ages of 8 to 10 days. Cochlear preparations were mounted under an Axioskope microscope (Zeiss, Oberkochem, Germany) and viewed with differential interference contrast using a 63× water immersion objective and a camera with contrast enhancement (Hamamatsu C2400-07, Hamamatsu Corporation, Bridgewater, NJ). Methods for whole cell patch clamp of inner hair cells were as described previously (*29*, *30*). Briefly, inner hair cells were identified visually, by the size of their capacitance and by their characteristic voltage dependent Na^+ and K^+ currents, including at older ages a fast activating K^+-conductance. Some cells were removed to access inner hair cells, but mostly the pipet moved through the tissue with positive fluid flow used to clear the tip. The extracellular solution was 155 mM NaCl, 5.8 mM KCl, 1.3 mM $CaCl_2$, 0.9 mM $MgCl_2$, 0.7 mM NaH_2PO_4, 5.6 mM D-glucose, and 10 mM HEPES, pH 7.4. The pipet solution was 150 mM KCl, 3.5 mM $MgCl_2$, 0.1 mM $CaCl_2$, 10 mM BAPTA, 5 mM HEPES, 2.5 mM Na_2ATP, pH 7.2. Glass

[1] Abbreviations: α-ImI, alpha-conotoxin ImI; α-RgIA, alpha-conotoxin RgIA; BAPTA-AM, 1,2-bis(2-aminophenoxy)ethane-*N*,*N*,*N*′,*N*′-tetraacetic acid-acetoxymethyl ester; *n*H, Hill slope.

pipets (1.2-mm inner diameter) had resistances of 7−10 MΩ. Cells were maintained at a holding potential of −90 mV. Postsynaptic currents caused by the spontaneous release of ACh from efferent synaptic terminals contacting inner hair cells were occasionally observed. Therefore, to study the effect of the toxin on synaptic currents in these cells, transmitter release from efferent endings was accelerated by depolarization using 25 mM or 40 mM external potassium saline. In this case, the pipet solution was 150 mM KCl, 3.5 mM $MgCl_2$, 0.1 mM $CaCl_2$, 5 mM EGTA, 5 mM HEPES, 2.5 mM Na_2ATP, pH 7.2. 60 μM ACh (the EC50 in this preparation). Elevated potassium, plus or minus α-RgIA, or 60μM ACh (the EC_{50} in this preparation), also plus or minus toxin, or α-RgIA alone, were applied by a gravity-fed multichannel glass pipet (150-μm tip diameter) positioned about 300 μm from the recorded inner hair cell. All toxin solutions also contained 0.1 mg/mL bovine serum albumin to reduce nonspecific adsorption of peptide. The extracellular solution in these experiments was similar to that described above, except that $MgCl_2$ was omitted, and the $CaCl_2$ concentration was lowered to 0.5 mM to optimize the experimental conditions for measuring currents flowing through the α9α10 receptors (*29*). To minimize the contribution of SK channel currents, 1 nM apamin, a specific SK channel blocker, was added to the external working solutions. Currents in inner hair cells were recorded in the whole-cell patch clamp mode using an Axopatch 200B amplifier low pass filtered at 2−10 kHz and digitized at 5−20 kHz with a Digidata 1200 board (Axon Instruments, Union City, CA). Recordings were made at room temperature (22−25 °C). Voltages were not corrected for the voltage drop across the uncompensated series resistance. To determine the concentration dependence of α-RgIA block of ACh gated currents, different concentrations of the toxin were preapplied to the preparation for 10 min prior to coapplication of the same concentration of drug and ACh. The average peak amplitude of three control responses just prior to toxin exposure was used to normalize the amplitude of each test response elicited by ACh in the presence of the toxin.

Data Analysis. To generate concentration dependence curves for inhibition by conotoxins the percent responses to ACh measured at a range of [toxin] were fit, using Prism software (GraphPad), to the below equation where *n*H is the Hill coefficient and IC_{50} is the toxin concentration causing half-maximal block.

$$\% \text{ reponse} = 100/(1 + [\text{toxin}]/IC_{50})^{nH}$$

Statistical significance was evaluated by Student's *t* test (two-tailed, unpaired samples). A $p < 0.05$ was considered significant.

RESULTS

PCR-Based Discovery of α-RgIA. PCR amplification with *C. regius* DNA as template was used to generate a fragment of the α-RgIA gene that includes the region encoding the mature toxin. The gene fragment and theoretical translation product are shown in Figure 1. The putative sequence of mature α-RgIA was deduced by the presence of the stop codon at the C-terminal of the toxin precursor and the arginine residue indicated in Figure 1, which is assumed to define the proteolytic cleavage site that releases the mature toxin. Cleavage at this position is supported by the example of α-conotoxin α-ImI; the α-ImI precursor has an arginine at the same relative position as the putative cleavage site arginine of α-RgIA (*22*), and in this case the cleavage site has been confirmed by sequencing of α-ImI peptide isolated from venom (*25*).

α-RgIA Is a Specific Inhibitor of Xenopus Oocyte Expressed Rat α9α10 nAChRs. The ability of α-RgIA to inhibit ACh gated currents through oocyte-expressed nAChRs was measured. α-RgIA was tested on the rat α7, α2β2, α2β4, α3β2, α3β4, α4β2, α4β4, and α9α10 subtypes. It was also tested on a model for the α6β2β3 subtype, i.e., the previously described (*27*) rat α6/α3β2β3 receptor that contains a chimeric α6/α3 subunit in which the extracellular ACh binding domain is from the α6 subunit and the rest of the molecule is from the α3 subunit. This model receptor was used because it is functionally expressed in oocytes much better than native α6β2β3 channels.

As can be seen in Figure 2 and Table 1, α-RgIA inhibited the α9α10 nAChR subtype with an IC_{50} of approximately 5 nM. α9α10 receptors conduct large amounts of Ca^{2+} and thus activate significant Ca^{2+} gated Cl^- currents in oocytes (*15*). Thus, the block of α9α10 currents by α-RgIA was measured using both oocytes that had been equilibrated with a Ca^{2+} chelator and also, to ensure consistency with the non-α9α10 data, untreated oocytes. As can be seen in Table 1, Ca^{2+} chelation caused no difference in the block by α-RgIA, therefore the α9α10 inhibition curve in Figure 2 includes both sets of data (i.e. with and without chelator). α-RgIA showed about 1000-fold greater potency on the α9α10 receptor than on the closely related α7 receptor. α-RgIA was also at least 2000-fold more potent on α9α10 channels than on α2β2, α2β4, α3β4 , α3β2, α4β2, α4β4 and α6/α3β2β3, channels. The high degree of α-RgIA discrimination between the α9α10 and α3β2 subtypes is in contrast to the minimal (3-fold) difference in potency observed with the previously characterized α9α10 antagonist α-conotoxin PeIA (*23*).

α-RgIA Inhibits Native α9α10 Receptors. Cochlear hair cells are the main targets of descending cholinergic olivocochlear efferent fibers, and the efferent fiber-hair cell synapse is most likely mediated by postsynaptic α9α10 nAChRs (*13*−*15*). As shown in Figure 3, α-RgIA potently blocked currents evoked by exogenous application of ACh to inner hair cells. The IC_{50} value obtained (6.6 nM with a 95% confidence interval of 4.20 nM to 10.4 nM) matches that obtained on oocyte expressed α9α10 channels confirming the presence of α9α10 nAChRs on the hair cells and indicating that oocyte expressed α9α10 receptors are a reliable model for the native channels.

ACh mediated synaptic transmission is very different from experimental application of ACh to oocytes or excised pieces of the organ of Corti. At synapses transmitter is released into the synaptic cleft in very close proximity to postsynaptic receptors and reaches millimolar concentrations (*12*). Therefore the effect of α-RgIA in a more physiologically relevant model was studied by promoting synaptic ACh release in isolated organs of Corti using high KCl concentrations. As shown in Figure 4, 30 nM α-RgIA blocked responses to synaptically released ACh, indicating that the toxin is a valuable tool for inhibition of in vivo responses mediated by α9α10 nAChRs. Figure 4A shows K^+-evoked synaptic currents either in the absence or presence of α-RgIA. The

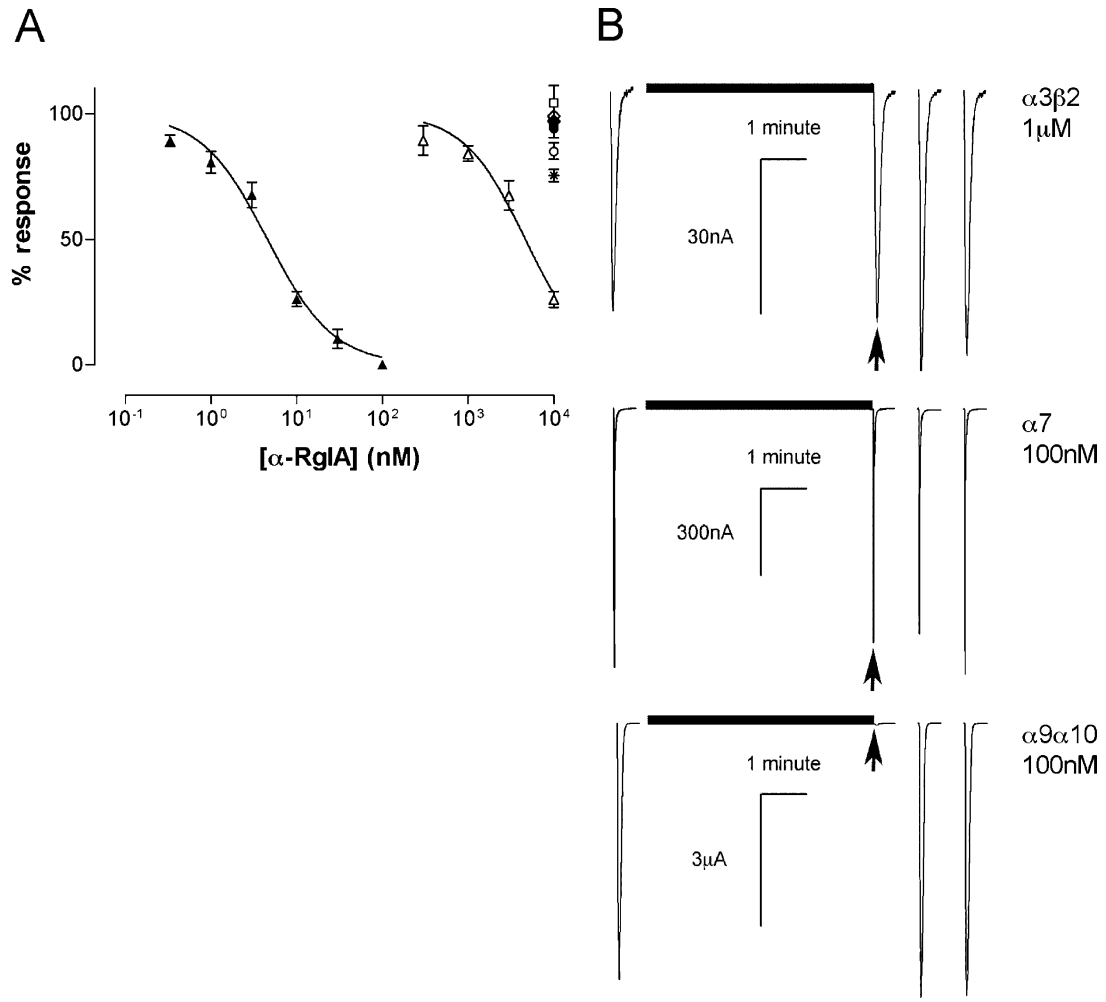

FIGURE 2: α-RgIA is a subtype specific inhibitor of oocyte expressed α9α10 nAChRs. A. Inhibition curves were obtained by static bath applications of various concentrations of α-RgIA to voltage clamped *Xenopus* oocytes expressing various nAChR subtypes (α7, white triangles; α9α10, black triangles; α2*β*2, black squares; α2*β*4, white squares; α3*β*2, black circles; α3*β*4, white circles; α4*β*2, black diamonds; α4*β*4, white diamonds; α6/α3*β*2*β*3, asterisks). The data points are the mean (± the SEM for at least 3 repetitions). B. Representative examples of the effects of α-RgIA on ACh-evoked currents of oocytes expressed nAChRs. The arrows point to the first ACh gated current obtained following application of the indicated α-RgIA concentrations to the indicted nAChR subtypes. Toxin application is represented by the black bars. As can be seen, 100 nM α-RgIA will cause almost complete block of the rat α9α10 subtype but has no effect on the closely related α7 subtype or the α3*β*2 subtype. As illustrated for the α9α10 receptor, on all subtypes where antagonism by α-RgIA was seen the inhibition was fully reversed 1 min after toxin washout.

Table 1: IC_{50} Values and Hill Slopes (*n*H) for Inhibition of Rat nAChRs by α-RgIA

nAChR subtype	IC_{50} (95% confidence interval); *n*H (95% confidence interval)
α2*β*2	>10 *μ*M; not determined
α2*β*4	>10 *μ*M; not determined
α3*β*2	>10 *μ*M; not determined
α3*β*4	>10 *μ*M; not determined
α4*β*2	>10 *μ*M; not determined
α4*β*4	>10 *μ*M; not determined
α7	4.66 *μ*M (3.66−5.94 *μ*M); 1.2 (0.84−1.6)
α6/α3*β*2*β*3	>10*μ*M; not determined
α9α10 (plus BAPTA)	5.19 nM (4.14 nM-6.50 nM); 1.2 (0.94−1.5)
α9α10 (minus BAPTA)	3.60 nM (2.62−4.95 nM); 0.98 (0.70−1.3)
α9α10 (all data)	4.55 nM (3.79−5.46 nM); 1.1 (0.92−1.3)

observed block was rapidly reversed after toxin was washed out of the preparation. α-RgIA caused a reduction ($p < 0.0001$) in the amplitude of the synaptic currents (Figure 4B) from 54.2 pA (95% confidence interval, 51.5 to 56.9 pA; number of events, 363; number of cells, 5) to 33.4 pA (95% confidence interval, 29.5 to 33.2 pA; number of events, 107; number of cells, 5). This result confirms the postsynaptic effect of the toxin on the nAChRs present in cochlear hair cells.

The C-Terminal Portion of α*-RgIA Confers* α9α*10 Specificity*. Residues 1 to 8 of the previously characterized (*25*) α4/3 conotoxin α-ImI are identical to those in α-RgIA; however, there are a number of differences (highlighted in Table 2) in the rest of the molecule. To explore the significance of these differences α-ImI was tested on the α9α10 subtype and was found to block this subtype with much less potency than α-RgIA. The IC_{50} was only about 2 *μ*M as opposed to about 5 nM for α-RgIA (Figure 5). Thus the amino acid sequence in the C-terminal portion of α-RgIA contributes significantly to its high affinity block of α9α10 nAChRs.

DISCUSSION

By using conserved sequence found within the genes that encode α-conotoxin precursors, a PCR based technique was used to identify a novel peptide from the worm hunting *Conus* species *Conus regius*. Because the peptide was not

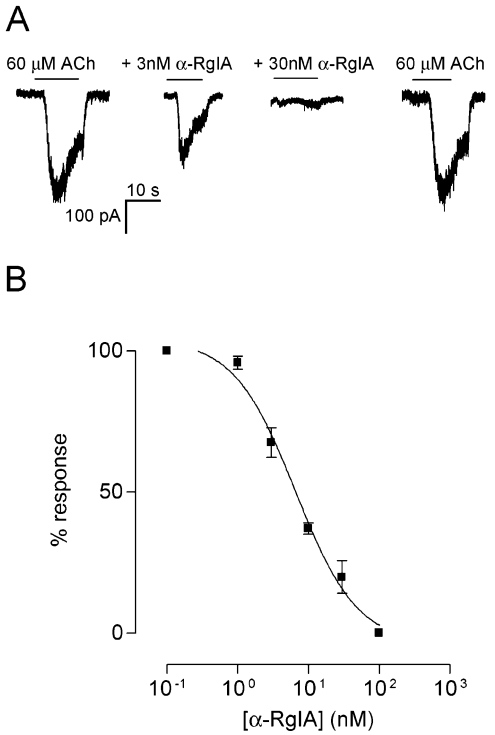

FIGURE 3: Effect of α-RgIA on ACh-evoked currents of inner hair cells. A. Representative currents evoked by 60 μM ACh alone, in the presence of 3 and 30 nM α-RgIA following preapplication of the same concentration of peptide, and after peptide washout (right-hand trace). B. The concentration dependence of α-RgIA inhibition of ACh evoked currents. The peak currents recorded after coapplication of ACh and toxin, following 10 min preapplication of the same concentration of toxin, are expressed as percentages of peak currents recorded in the absence of toxin. Each data point is the mean (± the standard error of the mean) of recordings from four to six cells. The IC_{50} obtained was 6.6 nM (95% confidence interval: 4.20 nM to 10.4 nM), and the Hill slope was 1.0 (95% confidence interval: 0.6 to 1.4).

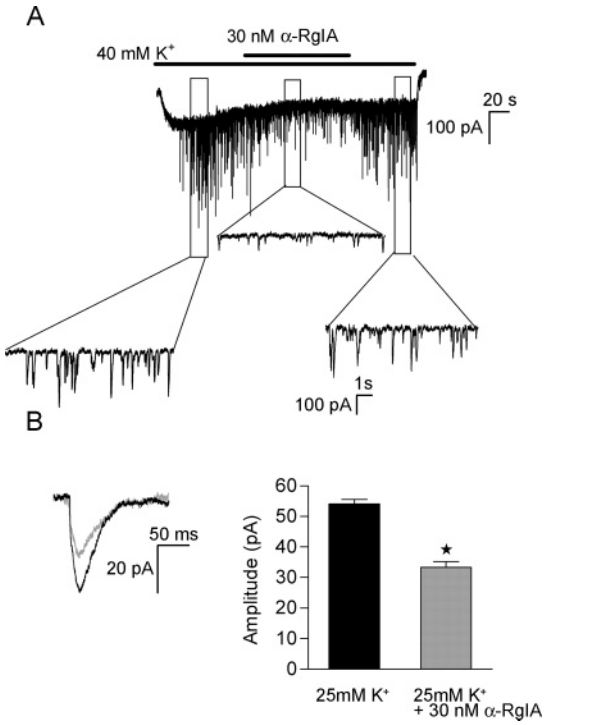

FIGURE 4: Effect of α-RgIA on inner hair cell synaptic currents. A. Representative example of the effect of 30 nM α-RgIA on postsynaptic currents evoked by 40 mM KCl. The insets show postsynaptic currents on an expanded time scale. B. Left: Superimposed averages of synaptic currents evoked by 25 mM KCl either alone (black) or in the presence of 30 nM α-RgIA (gray). Right: Bar diagram showing the effect of 30 nM α-RgIA on the amplitude of postsynaptic currents evoked by 25 mM KCl. The recordings are from 5 independent inner hair cells, and the number of analyzed events was 363 and 107, in the absence and presence of α-RgIA, respectively. The star denotes a significant difference, $p < 0.0001$. The reduction of the amplitude of the synaptic currents was from −54.2 pA (95% confidence interval: 51.5 to 56.9 pA) to −33.4 pA (95% confidence interval: 29.5 to 33.2 pA).

isolated from snail venom, it is not possible to rule out the possibility that the native molecule has posttranslational modifications that were not incorporated in the synthetic α-RgIA used in this study. Nevertheless, the synthetic molecule was found to be a potent and specific inhibitor of the α9α10 nAChR subtype. The ability of α-RgIA to discriminate between α9α10 and α3β2 receptors is unique given that the only other described α-conotoxin inhibitor of the α9α10 subtype (α-PeIA) is also a potent blocker of α3β2 channels (*23*).

Since α-PeIA does not discriminate between α3β2 and α9α10 nAChRs (*23*) but α-RgIA does, it could be a valuable probe of nAChR function in tissues where both the α9α10 and α3β2 receptors potentially occur. For example in neurons of the dorsal root ganglion α3, β2, α9, and α10 mRNAs have been detected by RT PCR and in situ hybridization (*17*, *31*). Extraneuronal locations where α9α10 and α3β2 nAChR expression may overlap have also been described; α3 and β2 subunit mRNAs have been detected in two lymphocyte models (peripheral mononuclear leukocytes and leukemic cell lines) (*32*), and α9 and α10 expression has been also detected in purified lymphocyte populations (*18*). Additionally, in skin keratinocytes from knockout mice lacking the α7 subunit, α9α10 nAChRs were up-regulated along with α3 containing channels that lack the α5 subunit, i.e., potentially α3β2 channels (*19*).

Table 2: Properties of Characterized α4/3 Conotoxins

conotoxin	sequence	species (prey)	subtype specificity	ref
α-ImI	GCCSDPRCAWRC#[a]	*C. imperialis* (worm)	α3β2,α7	*34*
α-RgIA	GCCSDPRCRYRCR	*C. regius* (worm)	α9α10	this study
α-ImII	ACCSDRRCRWRC#[a]	*C. imperialis* (worm)	α7, α1β1$\delta\epsilon$	*22*, *34*

[a] The symbol "#" represents C-terminal amidation. Residues in α-ImI and α-ImII that differ from the residue at the corresponding position in α-RgIA are underlined.

α-RgIA blocks currents mediated by hair cell α9α10 nAChRs gated with exogenously applied ACh as well as synaptically released ACh (Figures 3 and 4). This confirms that α-RgIA is a valuable tool for antagonism of α9α10 receptors in vivo and in biological preparations containing the α9α10 receptor.

The inter-cysteine spacing of α-RgIA places it in the α4/3 subfamily of conotoxins (i.e. in a family of peptides with four amino acids in the first loop and three in the second loop). Thus, to our knowledge, α-RgIA is the third α4/3 peptide in the literature (see Table 2): all are from worm hunting snails, and no α4/3 peptides have been reported in fish or mollusk hunting cones. An intriguing possibility is that α4/3 toxins are a specialization of worm hunting snails

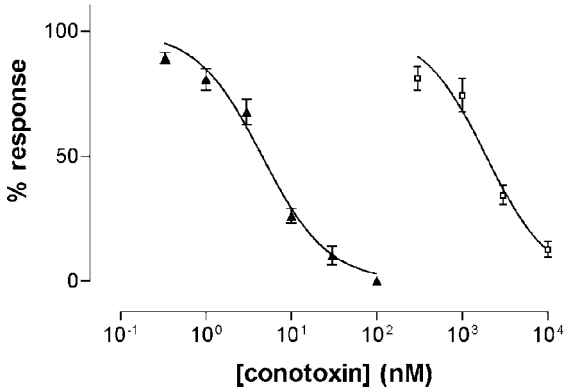

FIGURE 5: Comparison of block of α9α10 channels by α-RgIA and α-ImI. Inhibition curves were obtained by static bath applications of various concentrations of α-RgIA (black triangles) and α-ImI (white squares) to voltage clamped *Xenopus* oocytes expressing α9α10 nAChRs. The data points are the mean (± the SEM for at least 3 repetitions). The data for α-RgIA is the same as in Figure 2. The inhibition by α-ImI has an IC_{50} of 1.91 μM (95% confidence interval: 1.47 μM to 2.47 μM) and a Hill slope of 1.2 (95% confidence interval: 0.80 to 1.6). As with α-RgIA (see Figure 2), α-ImI block of the α9α10 channel was fully reversed 1 min after washout of toxin.

and evolved to target receptors specific to the prey, predators, and/or competitors of these snails.

An additional common feature of the three α4/3 toxins characterized to date is that they all potently inhibit α7 or α9α10 receptors, thus the native targets of these peptides may be related to α7 and/or α9α10 receptors from vertebrates. Identification and characterization of members of this subfamily of toxins could therefore be a particularly valuable way to identify antagonists of nAChRs containing only alpha subunits.

Comparison of the α-ImI sequence with the sequences of two previously characterized α4/3 toxins (Table 2) reveals that α-ImII and α-RgIA differ along their entire lengths but α-ImI and α-RgIA diverge only in their C-terminal halves. To investigate the significance of the C-terminal halves of α4/3 conotoxins on α9α10 potency, α-ImI was tested on the α9α10 subtype and was found to be a much less potent antagonist of this receptor than α-RgIA (Figure 5). Thus features of the R9, Y10, R13 triad of α-RgIA contribute significantly to its high affinity block of α9α10 nAChRs. In addition, α-ImI is a more potent inhibitor of the α3β2 and α7 nAChRs than α-RgIA (the respective IC_{50} values of α-ImI and α-RgIA on the rat α3β2 subtype are approximately 165 nM (unpublished observation) and >10 μM (Table 1), and on rat α7 channels they are approximately 200 nM (*22*) and 5 μM (Table 1)). Thus the residues in the C-terminal portion of α-RgIA are also responsible for the specificity as well as potency of the α9α10 block (i.e. the lack of potency against the α3β2 and α7 subtypes as well as the high potency for the α9α10 subtype). The observed block of the rat α3β2 subtype by α-ImI is at odds with a previous report (*33*) that described no inhibition of rat α3β2 channels by this toxin (in this case nAChRs were gated by 20 s pulses of 500 μM ACh), but is consistent with a report describing potent block of currents gated by short (1 s) ACh pulses applied to the human α3β2 channel (*34*).

In conclusion, α-RgIA is a potent and specific inhibitor of oocyte expressed and native α9α10 nAChRs. Comparison of the α-RgIA sequence with that of the similar α4/3 peptide α-ImI reveals that the amino acids toward the C-terminal of α-RgIA are important determinants of its preferential α9α10 receptor antagonism.

REFERENCES

1. Armishaw, C. J., and Alewood, P. F. (2005) Conotoxins as research tools and drug leads, *Curr. Protein Pept. Sci. 6*, 221−40.
2. Wang, C. Z., and Chi, C. W. (2004) Conus peptides—a rich pharmaceutical treasure, *Acta Biochim. Biophys. Sin. 36*, 713−23.
3. Livett, B. G., Gayler, K. R., and Kahlil, Z. (2004) Drugs from the sea: conopeptides as potential therapeutics, *Curr. Med. Chem. 11*, 1715−23.
4. Lewis, R. J. (2004) Conotoxins as selective inhibitors of neuronal ion channels, receptors and transporters, *IUBMB Life 56*, 89−93.
5. Terlau, H., and Olivera, B. M. (2004) *Conus* venoms: a rich source of novel ion channel-targeted peptides, *Physiol. Rev. 84*, 41−68.
6. McIntosh, J. M., Santos, A. D., and Olivera, B. M. (1999) *Conus* peptides targeted to specific nicotinic acetylcholine receptor subtypes, *Annu. Rev. Biochem. 68*, 59−88.
7. Janes, R. W. (2005) alpha-Conotoxins as selective probes for nicotinic acetylcholine receptor subclasses, *Curr. Opin. Pharmacol. 5*, 280−92.
8. Dutton, J. L., and Craik, D. J. (2001) α-Conotoxins: nicotinic acetylcholine receptor antagonists as pharmacological tools and potential drug leads, *Curr. Med. Chem. 8*, 327−44.
9. Arias, H. R., and Blanton, M. P. (2000) Alpha-conotoxins, *Int. J. Biochem. Cell Biol. 32*, 1017−28.
10. Karlin, A. (2002) Emerging structure of the nicotinic acetylcholine receptors, *Nat. Rev. Neurosci. 3*, 102−14.
11. Gotti, C., and Clementi, F. (2004) Neuronal nicotinic receptors: from structure to pathology, *Prog. Neurobiol. 74*, 363−96.
12. Le Novere, N., Corringer, P. J., and Changeux, J. P. (2002) The diversity of subunit composition in nAChRs: evolutionary origins, physiologic and pharmacologic consequences, *J. Neurobiol. 53*, 447−56.
13. Sgard, F., Charpantier, E., Bertrand, S., Walker, N., Caput, D., Graham, D., Bertrand, D., and Besnard, F. (2002) A Novel Human Nicotinic Receptor Subunit, α10, That Confers Functionality to the α9-Subunit, *Mol. Pharmacol. 61*, 150−9.
14. Elgoyhen, A. B., Johnson, D. S., Boulter, J., Vetter, D. E., and Heinemann, S. (1994) α9: an acetylcholine receptor with novel pharmacological properties expressed in rat cochlear hair cells, *Cell 79*, 705−15.
15. Elgoyhen, A. B., Vetter, D. E., Katz, E., Rothlin, C. V., Heinemann, S. F., and Boulter, J. (2001) α10: a determinant of nicotinic cholinergic receptor function in mammalian vestibular and cochlear mechanosensory hair cells, *Proc. Natl. Acad. Sci. U.S.A. 98*, 3501−6.
16. Haberberger, R. V., Bernardini, N., Kress, M., Hartmann, P., Lips, K. S., and Kummer, W. (2004) Nicotinic acetylcholine receptor subtypes in nociceptive dorsal root ganglion neurons of the adult rat, *Auton. Neurosci. 113*, 32−42.
17. Lips, K. S., Pfeil, U., and Kummer, W. (2002) Coexpression of α9 and a10 nicotinic acetylcholine receptors in rat dorsal root ganglion neurons, *Neuroscience 115*, 1−5.
18. Peng, H., Ferris, R. L., Matthews, T., Hiel, H., Lopez-Albaitero, A., and Lustig, L. R. (2004) Characterization of the human nicotinic acetylcholine receptor subunit alpha (alpha) 9 (CHRNA9) and alpha (alpha) 10 (CHRNA10) in lymphocytes, *Life Sci. 76*, 263−80.
19. Arredondo, J., Nguyen, V., Chernyavsky, A. I., Bercovich, D., Orr-Urtreger, A., Kummer, W., Lips, K., Vetter, D. E., and Grando, S. A. (2002) Central role of alpha7 nicotinic receptor in differentiation of the stratified squamous epithelium, *J. Cell Biol. 159*, 325−36.
20. Nguyen, V. T., Ndoye, A., and Grando, S. A. (2000) Novel human alpha9 acetylcholine receptor regulating keratinocyte adhesion is targeted by Pemphigus vulgaris autoimmunity, *Am. J. Pathol. 157*, 1377−91.
21. Kurzen, H., Berger, H., Jager, C., Hartschuh, W., Naher, H., Gratchev, A., Goerdt, S., and Deichmann, M. (2004) Phenotypical and molecular profiling of the extraneuronal cholinergic system of the skin, *J. Invest. Dermatol. 123*, 937−49.
22. Ellison, M., McIntosh, J. M., and Olivera, B. M. (2003) α-Conotoxins ImI and ImII: similar α7 nicotinic receptor antagonists act at different sites, *J. Biol. Chem. 278*, 757−64.

23. McIntosh, J. M., Plazas, P. V., Watkins, M., Gomez-Casati, M. E., Olivera, B. M., and Elgoyhen, A. B. (2005) A novel α-conotoxin, PeIA, cloned from Conus pergrandis, discriminates between rat α9α10 and α7 nicotinic cholinergic receptors, *J. Biol. Chem. 280*, 30107−12.
24. Luo, S., Nguyen, T. A., Cartier, G. E., Olivera, B. M., Yoshikami, D., and McIntosh, J. M. (1999) Single-residue alteration in α-conotoxin PnIA switches its nAChR subtype selectivity, *Biochemistry 38*, 14542−8.
25. McIntosh, J. M., Yoshikami, D., Mahe, E., Nielsen, D. B., Rivier, J. E., Gray, W. R., and Olivera, B. M. (1994) A nicotinic acetylcholine receptor ligand of unique specificity, α-conotoxin ImI, *J. Biol. Chem. 269*, 16733−9.
26. Cartier, G. E., Yoshikami, D., Gray, W. R., Luo, S., Olivera, B. M., and McIntosh, J. M. (1996) A new α-conotoxin which targets α3β2 nicotinic acetylcholine receptors, *J. Biol. Chem. 271*, 7522−8.
27. Dowell, C., Olivera, B. M., Garrett, J. E., Staheli, S. T., Watkins, M., Kuryatov, A., Yoshikami, D., Lindstrom, J. M., and Mcintosh, J. M. (2003) α-Conotoxin PIA is selective for α6 subunit-containing nicotinic acetylcholine receptors, *J. Neurosci. 23*, 8445−52.
28. McIntosh, J. M., Gardner, S., Luo, S., Garrett, J. E., and Yoshikami, D. (2000) *Conus* peptides: novel probes for nicotinic acetylcholine receptor structure and function, *Eur. J. Pharmacol. 393*, 205−8.
29. Katz, E., Elgoyhen, A. B., Gomez-Casati, M. E., Knipper, M., Vetter, D. E., Fuchs, P. A., and Glowatzki, E. (2004) Developmental regulation of nicotinic synapses on cochlear inner hair cells, *J Neurosci. 24*, 7814−20.
30. Glowatzki, E., and Fuchs, P. A. (2000) Cholinergic synaptic inhibition of inner hair cells in the neonatal mammalian cochlea, *Science 288*, 2366−8.
31. Genzen, J. R., Van Cleve, W., and Mc Gehee, D. S. (2001) Dorsal root ganglion neurons express multiple nicotinic acetylcholine receptor subtypes, *J. Neurophysiol. 86*, 1773−82.
32. Sato, K. Z., Fujii, T., Watanabe, Y., Yamada, S., Ando, T., Kazuko, F., and Kawashima, K. (1999) Diversity of mRNA expression for muscarinic acetylcholine receptor subtypes and neuronal nicotinic acetylcholine receptor subunits in human mononuclear leukocytes and leukemic cell lines, *Neurosci. Lett. 266*, 17−20.
33. Johnson, D. S., Martinez, J., Elgoyhen, A. B., Heinemann, S. F., and McIntosh, J. M. (1995) α-Conotoxin ImI exhibits subtype-specific nicotinic acetylcholine receptor blockade: preferential inhibition of homomeric α7 and α9 receptors, *Mol. Pharmacol. 48*, 194−199.
34. Ellison, M., Gao, F., Wang, H.-L., Sine, S. M., Mcintosh, J. M., and Olivera, B. M. (2004) α-Conotoxins ImI and ImII target distinct regions of the human α7 nicotinic acetylcholine receptor and distinguish human nAChR subtypes, *Biochemistry 43*, 16019−26.

BI0520129